



## ADAPTIVE-PASSIVE NOISE CONTROL WITH SELF-TUNING HELMHOLTZ RESONATORS

J. M. DE BEDOUT, M. A. FRANCKEK, R. J. BERNHARD AND L. MONGEAU

*Department of Mechanical Engineering, Purdue University, West Lafayette, Indiana,  
47907, U.S.A.*

*(Received 26 February 1996, and in final form 4 October 1996)*

A tunable Helmholtz resonator and a novel feedback based control law that achieves optimal resonator tuning for time varying tonal noise control applications are presented in this paper. The proposed tuning strategy combines an open loop tuning algorithm based on a simple lumped parameter model of the resonator with a gradient descent approach based on a feedback control structure that ensures robust performance. Optimal tuning of the resonator is achieved despite system uncertainties such as variations in the excitation frequency and environmental changes. An experimental verification of the proposed control law is included. Sound pressure level reductions of up to 30 dB were achieved in an experimental duct system using a tunable Helmholtz resonator.

© 1997 Academic Press Limited

### 1. INTRODUCTION

Since ancient Greece [1], Helmholtz resonators have been exploited to enhance or attenuate sound fields. Helmholtz resonators have found use in reverberant spaces such as churches [2], as mufflers in ducts and pipes [3], and in many other applications. One advantage of the Helmholtz resonator is its simplicity. It is comprised of a cavity connected to the system of interest through one or several short narrow tubes. However, Helmholtz resonators must be tuned precisely to achieve significant noise attenuation. The frequency range over which Helmholtz resonators are effective is relatively narrow. Changes in the excitation frequency and environmental conditions influence the performance of these devices.

Due to the limitations of conventional passive devices such as Helmholtz resonators, active noise control methods utilizing adaptive digital filters have been the subject of considerable investigation. Usually, these schemes achieve noise reduction by loading or unloading the primary source, not by absorbing the energy [4]. The main advantage of active noise control over passive control schemes is the implicit adaptability of the control system to changing environments and excitations. Furthermore, complex signals including broadband noise can be significantly attenuated, provided that a reference signal can be utilized [5]. Unfortunately, active control of noise tends to become progressively more expensive as higher sampling frequencies and faster microprocessors are used to implement the control algorithms [6]. Additionally, since these control schemes are capable of adding energy into the system, there is the possibility of creating more noise if the system does not adapt successfully.

An emerging class of noise and vibration control solutions are adaptive-passive systems. Passive devices such as Helmholtz resonators and vibration absorbers can be enhanced with on-board intelligence to tune the passive parameters to ensure robust performance for changing conditions. The main advantages of using adaptive-passive devices over strictly active schemes are that additional energy is not required to achieve noise reduction

and that the control algorithms are simple. The principal advantage of adaptive-passive devices over purely passive solutions is that the devices remain tuned for changing environments and time-varying excitations.

### 1.1. PREVIOUS WORK IN ADAPTIVE-PASSIVE NOISE CONTROL

The investigation of adaptive-passive devices has grown over the past few years. The natural frequency of a Helmholtz resonator can be controlled by adjusting the resonator neck dimensions, cavity volume, or both. Therefore, adaptive Helmholtz resonators (and quarter wavelength resonators) can be used to attenuate noise over a bandwidth of excitation frequencies by utilizing mechanisms to change these dimensions. In recent years, several investigations have been performed to study the use of adaptive Helmholtz resonators for noise control applications in ducts and ventilation systems.

Koopman and Neise [7, 8] investigated the use of adjustable quarter-wavelength resonators to attenuate the blade passage frequency tone of centrifugal fans. Tuning of the resonators was achieved by changing the cavity length via a movable Teflon piston. Although no suggestions were given concerning the implementation of a controller to achieve the optimal tuning of the resonators, it was reported that the use of the adjustable resonators provided reductions in the blade passage frequency tones of up to 29 dB with no adverse effects on the fan performance.

Little *et al.* [9] proposed a fluidic Helmholtz resonator for use as an adaptive engine mount. Tuning of the resonator was to be achieved by changing the neck cross-sectional area, thereby varying the neck inertance of the device. A novel electro-rheological fluid valve was suggested to provide continuous tuning, as opposed to the discrete nature of the valves commonly used. However, a control scheme for tuning the resonator was not described.

Lamancusa [10] suggested the use of variable volume Helmholtz resonators as an alternative to expansion chamber mufflers in automobiles. Two variable volume resonator configurations were proposed. For the first design, the volume was continuously varied by displacing a piston inside the cavity. For the second configuration, several discrete volumes were utilized by manipulating closeable partitions within the cavity. The suggested tuning algorithm consisted of varying the resonator volume according to an engine r.p.m. signal. Although no experimental verification of this open loop control law was provided, it was found that manual tuning of the continuously variable volume resonator could provide insertion losses of more than 30 dB. Krause *et al.* [11, 12] have also experimented with variable volume and neck Helmholtz resonators to suppress noise in automotive tailpipes.

Matsuhisa *et al.* [13, 14] developed a resonator in which the volume was changed by displacing a piston within the cavity. Tuning of the resonator, which was used as a side branch in a duct, was achieved by comparing the phase of the sound pressure in the duct with that in the resonator cavity. The resonator cavity was adjusted such that the phase difference was 90 degrees, thereby achieving the antiresonance of the duct and resonator system. This implementation required three sensors: one microphone to measure the excitation frequency, one to measure the pressure in the duct, and another to measure the pressure in the cavity. This investigation reported reductions in sound pressure levels of 30 dB for a speaker driven system, and 20 dB for a fan driven system.

McDonald *et al.* [15] have been granted an international patent on an adaptive Helmholtz resonator for tonal noise control in duct systems that is tuned in a similar manner to Matsuhisa's [13, 14]. The adjustable resonator is adapted by simultaneously tuning the cavity volume and neck length according to the phase relationship between the pressure in the resonator cavity and the duct system.

Although adaptive Helmholtz resonators have been used previously, in most cases they were actuated either mechanically or through open loop schemes, with little or no attention given to robust tuning strategies. A tunable, variable volume Helmholtz resonator with a robust, simple control algorithm to achieve maximum performance is presented in this paper. The robust control algorithm developed for tuning the resonator is a combination of open loop control for coarse tuning, with closed loop control for precise tuning. The coarse tuning algorithm adjusts the resonator volume based on a lumped parameter model of the device. The precise tuning algorithm utilizes a gradient descent method based on a feedback control structure which minimizes the output voltage of a microphone.

2. ADAPTIVE-PASSIVE RESONATOR DESIGN

The behavior of a Helmholtz resonator is analogous to that of a lumped, single-degree-of-freedom system (see Figure 1). At low frequencies, such that the acoustic wavelength is much larger than the dimensions of the Helmholtz resonator, the cavity volume and neck dimensions of the resonator determine the natural frequency of the device. The volume of air in the neck of the Helmholtz resonator behaves like a mass and the volume of air in the cavity provides a reacting force analogous to that of a spring. The excitation is provided by tonal pressure fluctuations acting over the opening of the neck, resulting in oscillations of the volume of air in the neck. The natural frequency of a Helmholtz resonator, denoted as  $\omega_0$ , is given by

$$\omega_0 = c\sqrt{S/L_{eff}V}, \tag{1}$$

where  $S$  is the cross-sectional area of the neck,  $c$  is the speed of sound,  $V$  is the cavity volume of the resonator, and  $L_{eff}$  is the effective resonator neck length, which includes a correction factor for mass-loading due to air entrainment near the neck extremities [16].

The frequency response of a duct with a side branch Helmholtz resonator has a notch at the resonator natural frequency, making the resonator an acoustic band-stop filter. However, the bandwidth over which noise is attenuated is narrow, limiting conventional Helmholtz resonators to fixed frequency tonal noise suppression. This limitation can be removed by creating a tunable Helmholtz resonator, the natural frequency of which can be varied by altering the physical dimensions of the resonator.

The tunable Helmholtz resonator used in this investigation is a variable volume device. The resonator dimensions were chosen such that the tunable frequency range is 60–180 Hz. The largest dimension of the resonator was designed to be less than one quarter of the smallest wavelength to avoid standing waves within the device.

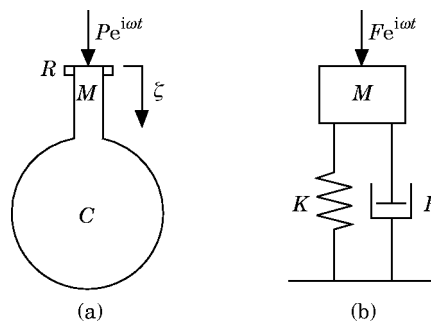


Figure 1. (a) A Helmholtz resonator. (b) A single-degree-of-freedom system.

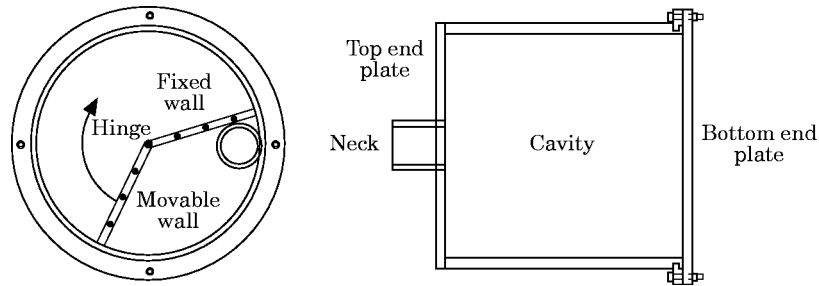


Figure 2. A variable volume Helmholtz resonator.

The variable volume actuation of the Helmholtz resonator is realized by rotating an internal radial wall inside the resonator cavity with respect to an internal fixed wall (see Figure 2). This configuration allows a continuously variable volume. The fixed wall is attached to the side of the cylinder and the top end plate of the resonator. The movable wall is fixed to the bottom end plate, which is free to rotate against the bottom face of the cylinder. This bottom plate is attached to a DC motor which provides the torque to change the volume. The fixed and movable walls are hinged together at the center of the cylinder.

To minimize the losses within the resonator, consideration was given to reducing the interaction between the two cavities produced by the two walls. A flexible membrane was attached to both walls along the hinge to seal the two cavities. Additionally, high vacuum stopcock grease was spread across the cylinder walls, to seal the small gaps between the wall edges and the cylinder.

The volume of the final design is bounded between  $1491 \text{ cm}^3$  and  $14\,093 \text{ cm}^3$ . The resonator cavity radius is  $15.1 \text{ cm}$ , and the cavity length is  $24.6 \text{ cm}$ . The thickness of the radial walls is  $0.95 \text{ cm}$ . The radius of the resonator neck is  $2.5 \text{ cm}$  and the neck length is  $8 \text{ cm}$ . The effective neck length of the resonator is contingent upon conditions at the exit of the neck. Since the resonator for this investigation is used as a side branch for a duct system, both ends of the neck are assumed to behave as flanged terminations.

For the purposes of this investigation, it was assumed that for any given wall position, the tunable Helmholtz resonator behaved like a conventional Helmholtz resonator with the same cavity volume and neck dimensions. This assumption disregards the effects of wall vibration and the interaction of the two cavities on the reactance of the resonator.

### 3. ROBUST TUNING CONTROL LAW DEVELOPMENT

The main objective of the tuning algorithm for an adaptive-passive device is to achieve and maintain the maximum attenuation of tonal noise in the system of interest under changing environments and excitation frequencies. The resonator tuning algorithm developed in this investigation consists of two tuning strategies: an open loop, coarse tuning scheme and a feedback gradient based precise tuning control law. Collectively, these individual strategies ensure robust attenuation performance of the passive device despite variations in the noise source frequency and environmental changes.

To justify this proposed tuning control law approach, consider the plot of the sound pressure level as a function of the resonator natural frequency shown in Figure 3. The noise source for this figure is an  $80 \text{ Hz}$  tone. The sound pressure level is measured at the microphone location downstream from the Helmholtz resonator, as shown below in Figure 4. A feedback based tuning algorithm could utilize the slope of the sound pressure versus

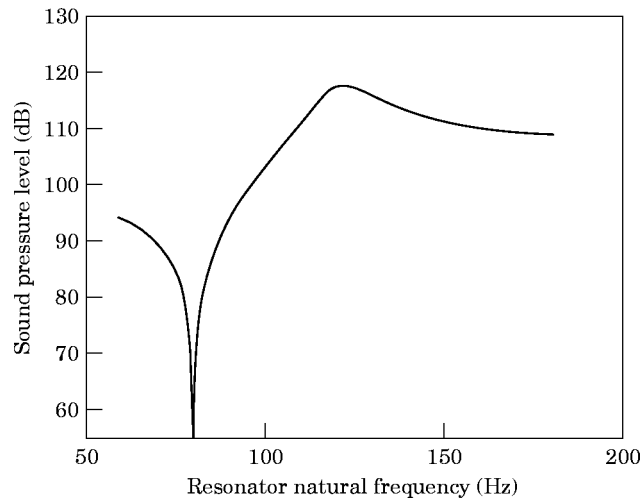


Figure 3. Sound pressure level versus natural frequency for constant excitation frequency of 80 Hz.

natural frequency curve to obtain a tuning direction for the resonator, and thus descend along the gradient of the curve until the minimum sound pressure is achieved. For the frequency range of the resonator, there are two minima of sound pressure level. The first minimum occurs at the resonator natural frequency of 80 Hz. This is the global minimum and the frequency to which the adaptive Helmholtz resonator should be tuned. The second minimum occurs above 180 Hz. This minimum is a local minimum for the sound pressure level. A tuning strategy strictly based on a gradient descent approach would not have a mechanism to distinguish the difference between these two minima and hence performance optimization would not be guaranteed. However, if an open loop tuning control law is used to first preset the resonator natural frequency so that the gradient based approach is guaranteed to converge to the global minimum, then optimal performance can be achieved. This is the basis upon which the tuning control law was developed.

### 3.1. EXPERIMENTAL FACILITY

The experimental facility and controller instrumentation are shown in Figure 4. Tonal noise is generated from a 10.2 cm diameter loudspeaker, enclosed in PVC tubing. The back

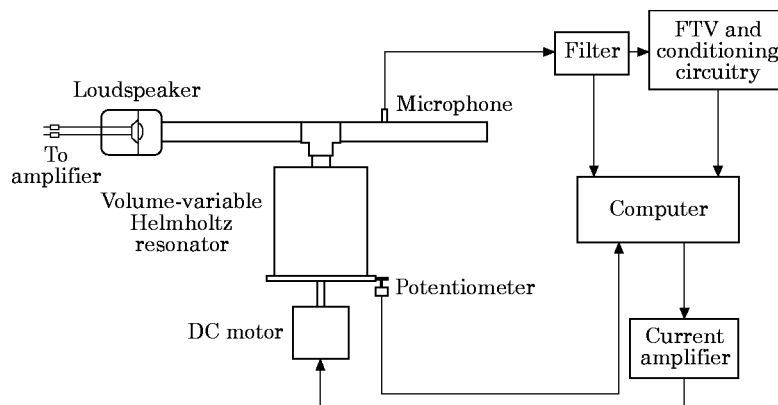


Figure 4. The experimental facility and controller instrumentation.

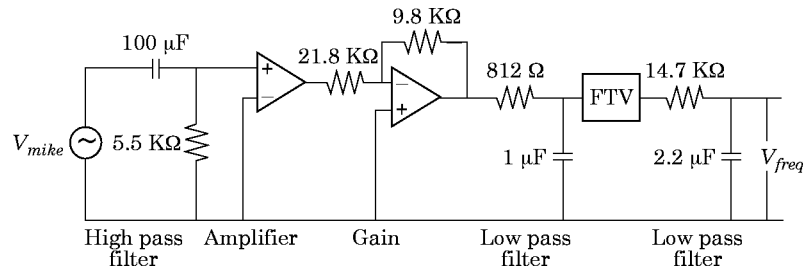


Figure 5. The conditioning circuitry for FTV excitation frequency determination.

cavity volume of the speaker enclosure is  $1140 \text{ cm}^3$ . The  $10.2 \text{ cm}$  diameter tubing extends  $10 \text{ cm}$  beyond the speaker face and is then reduced to a  $5 \text{ cm}$  diameter duct manufactured from PVC tubing. The duct is comprised of a  $62 \text{ cm}$  long section that connects the loudspeaker enclosure to the tunable Helmholtz resonator via a standard PVC T-coupling. A  $34 \text{ cm}$  long section of duct is extended from the T-coupling to an open unflanged termination.

A Brüel and Kjær type 4130  $1/2$  in condenser microphone is located downstream from the tunable Helmholtz resonator. The microphone voltage is processed through a four-pole Butterworth low pass filter with a  $190 \text{ Hz}$  cut-off frequency to remove high frequency noise. This filtered signal is used directly by the controller to determine the sound pressure magnitude in the duct. The wall position is measured by a ten-turn,  $5 \text{ K}\Omega$  potentiometer geared to the back plate of the tunable Helmholtz resonator. A full sweep of the resonator frequency range causes nine turns of the potentiometer.

The final input to the controller is a DC signal proportional to the excitation frequency. This signal is generated by a 451J Analog Devices frequency to voltage converter (FTV) and some additional signal conditioning circuitry (see Figure 5). The filtered AC signal from the microphone is first sent through a high pass filter with a  $0.3 \text{ Hz}$  cut-off frequency to remove DC offset. The signal is then passed through a high gain amplifier which clips the waveform, creating a constant amplitude square wave of the same frequency as the waveform from the microphone. The magnitude of the square wave is reduced by half, to satisfy the input voltage range of the frequency to voltage converter. This square wave is then sent through a low pass filter with a cut-off frequency of  $190 \text{ Hz}$  to smooth the waveform before entering the frequency to voltage converter. The frequency to voltage converter produces a DC voltage that is proportional to the frequency of the smoothed square wave, and thus proportional to the frequency of the filtered microphone signal. The output of the frequency to voltage converter is sent through a low pass filter with a  $30 \text{ Hz}$  cut-off frequency to remove the ripple voltage superimposed on the DC signal. This signal is then sent to the controller.

Since the focus of this investigation was on using the adaptive Helmholtz resonator to attenuate tonal noise, no consideration was given to the effect of additional simultaneous tonal frequencies on the frequency determination scheme. Helmholtz resonators should only be used for single frequency noise attenuation. Additional tonal noise components simultaneously occurring with the noise tone of interest will not be filtered out by the high pass or low pass filters if they are within the operating frequency band for the resonator, and could therefore cause problems for the frequency to voltage converter.

Other frequency determination schemes could be used in this proposed tuning control law. For example, the frequency could be measured by counting the number of zero-crossings of the microphone signal for a fixed time duration [17, 18]. Calculating the

excitation frequency based on source characteristics may also be possible for applications where the noise source has measurable parameters, such as a speed signal.

The controller was realized using a Compaq Prolinea 486 DX2 66 MHz tower computer and Keithley Metrabyte 12-bit data acquisition boards. The sampling rate used by the controller was 8600 Hz. The control logic was written in QuickBASIC 4.50. The controller output was first sent to a current amplifier, and then to a Dayton 4Z530 1/15 HP DC motor with a 267:1 gear reduction. The torque from this motor was used to adjust the resonator wall angle.

### 3.2. OPEN LOOP TUNING ALGORITHM

The objective of the open loop tuning algorithm is to preset the resonator natural frequency within the vicinity of the excitation frequency to ensure the convergence of the closed loop gradient descent algorithm. To accomplish this, the frequency of the noise source is estimated from the frequency to voltage converter signal. The open loop controller then drives the DC motor to rotate the interior wall to a position in which the theoretical resonator natural frequency is close to the estimated excitation frequency.

The natural frequency of the resonator as a function of the interior wall position can be derived from equation (1). The relationship between the resonator natural frequency and the angle between the two cavity walls is

$$\theta_{wall} = \frac{360}{\pi R_{cav}^2 L_{cav}} \left( \frac{S}{L_{eff} (2\pi f_o / c)^2} + V_{wall} \right), \quad (2)$$

where  $\theta_{wall}$  is the interior wall position in degrees,  $f_o$  is the desired resonator natural frequency in Hz,  $R_{cav}$  is the resonator cavity radius in cm,  $L_{cav}$  is the resonator cavity length in cm, and  $V_{wall}$  is the volume in  $\text{cm}^3$  subtracted from the resonator cavity volume due to the thickness of the walls.

Shown in Figure 6 is a comparison between equation (2) and measured discrete wall positions of optimal performance as a function of resonator natural frequency. Shown in Figure 7 is the difference between the measured discrete natural frequencies and those used in equation (2). As shown in Figure 7, the largest discrepancy between the predicted and

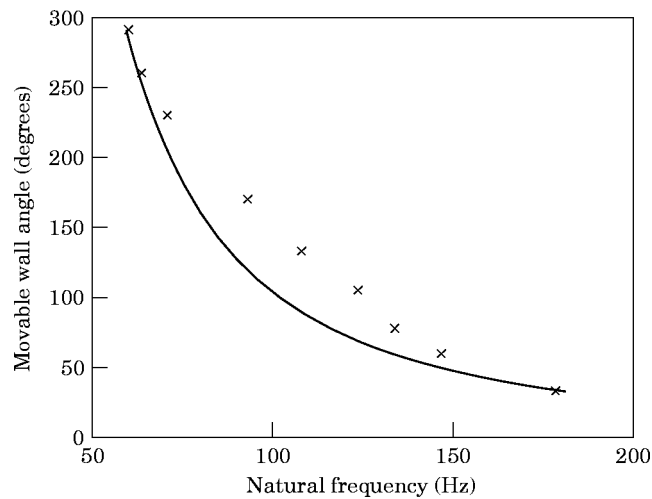


Figure 6. Theoretical and measured wall angles as a function of natural frequency. —, Predicted; ×, measured.

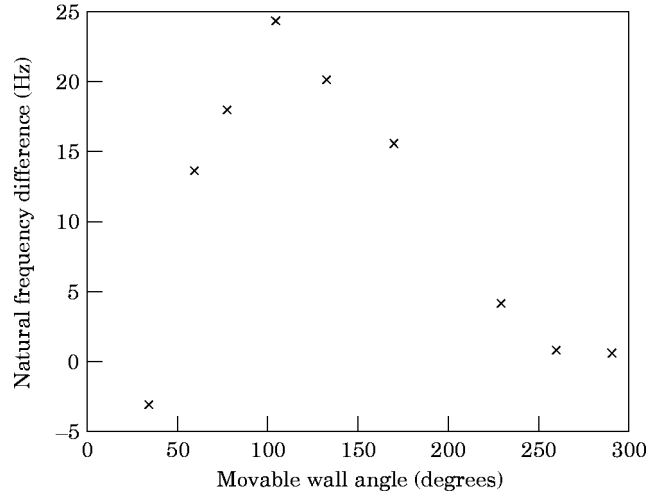


Figure 7. The difference between predicted and measured natural frequencies as a function of wall angle.

measured natural frequency is about 25 Hz at a natural frequency of 124 Hz. The error incurred in predicting the Helmholtz resonator natural frequency with equation (2) is the result of the simplified model used to represent the Helmholtz resonator. The accuracy of the model could be substantially improved by taking into account the effects of wall vibration and cavity interaction within the resonator cavity due to seal leakage and other sources. However, the model would still be susceptible to uncertainty due to environmental conditions, since the resonator natural frequency is dependent on the speed of sound. Therefore, there would always be a certain degree of inaccuracy involved when using analytical models. The use of such models as the sole means of tuning an adjustable resonator should therefore be discouraged.

In general, other approaches to developing a relationship between the tunable characteristic of the resonator and the resulting natural frequency can be used as appropriate. For example, a curve fit relating the natural frequency to wall angle can be generated experimentally. The only criterion to be satisfied in developing a relationship between the tunable characteristic of the resonator and the resonator natural frequency is that the calculated natural frequency must be sufficiently close to the real natural frequency to ensure convergence of the gradient based feedback controller to the global optimum.

The transfer between the open loop coarse tuning algorithm and the closed loop precise tuning algorithm occurs when

$$|\hat{f}_o - \hat{f}_{noise}| \leq \delta_T \text{ Hz}, \quad (3)$$

where  $\hat{f}_o$  is the predicted resonator natural frequency,  $\hat{f}_{noise}$  is the estimated excitation frequency, and  $\delta_T$  denotes a specified tolerance contingent upon model accuracy.  $\delta_T$  is selected using information about the Helmholtz resonator and duct system resonance and antiresonance. Shown in Figure 8 is a plot of the theoretical duct and resonator system antiresonance as a function of the excitation frequency and the Helmholtz resonator natural frequency. The theoretical system antiresonance follows a 45 degree line between the excitation frequency and the Helmholtz resonator natural frequency, indicating that the resonator is always tuned when its natural frequency is equal to the excitation frequency. Also shown are the actual measured resonance and antiresonance data from measured sound pressure spectra of the system. Notice that the resonance ridge exists only



between approximately 70 and 100 Hz. The minimum separation between the measured resonance and the theoretical antiresonance is 6.3 Hz, which occurs at an excitation frequency of 71 Hz. Recall that the Helmholtz resonator natural frequency must be on the appropriate side of the resonance to ensure the convergence of the closed loop gradient based algorithm. Therefore, the open loop algorithm must place the resonator natural frequency within less than 6.3 Hz of the theoretical natural frequency to ensure the closed loop convergence to the real antiresonance. The  $\delta_T$  value used in this investigation was 2 Hz, to give the controller a margin of safety.

### 3.3. GRADIENT BASED FEEDBACK TUNING CONTROL LAW

Environmental changes, variations in the excitation, and the inability to precisely identify the resonator natural frequency through acoustic models limits the performance potential of an open loop strategy. The gradient based tuning control law is employed for precise tuning of the resonator.

The gradient based tuning control law operates on the change in microphone voltage amplitude due to a change in the interior wall position. The algorithm starts by making 1 Hz incremental changes in the resonator natural frequency. The resulting change in the amplitude of the microphone voltage is measured. The gradient is calculated as

$$\nabla = \frac{M_i - M_{i-1}}{\hat{f}_{o_i} - \hat{f}_{o_{i-1}}}, \quad (4)$$

where  $M$  is the microphone voltage amplitude and  $i$  is a data sample counter. When there is a sign change in the gradient, the controller reverses tuning direction and changes the increment quantity in the resonator natural frequency to 0.7 Hz. Each time the minimum is passed, the controller reverses direction, and every time the slope changes from negative to positive, the increment quantity is decreased by 0.3 Hz. The minimum is passed in this manner a total of six times with a final increment quantity of 0.1 Hz. Once the final sign change is detected, the gradient based tuning is complete. This limitation of the search is used to avoid control chattering of the resonator.

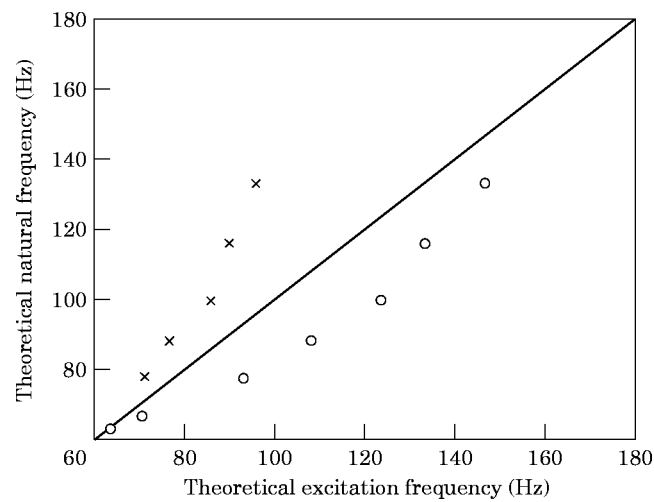


Figure 8. A plot of the system resonance and antiresonance in the resonator operating range: —, theoretical antiresonance; ○, measured antiresonance; ×, measured resonance.

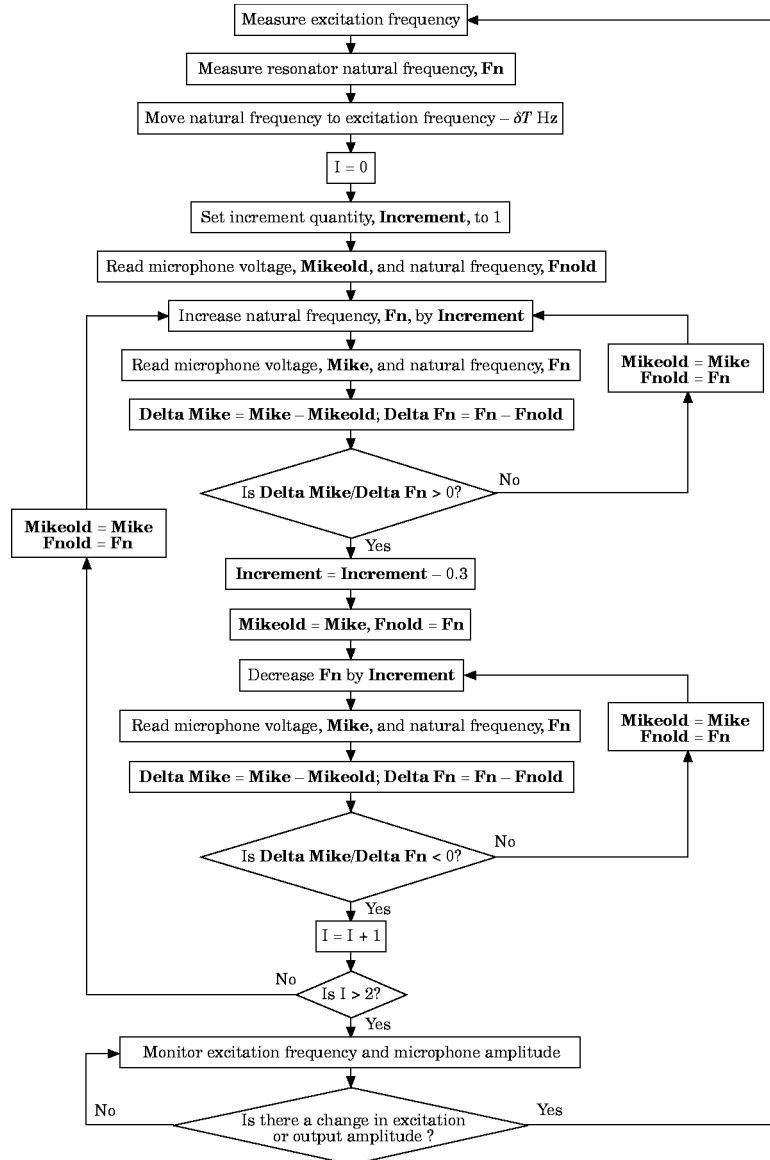


Figure 9. A logic flowchart of the control algorithm.

For this implementation, the speed of tuning is held constant throughout the tuning process. For other implementations, the speed of tuning could be made inversely proportional to the gradient of the sound pressure versus natural frequency curve. This would provide faster tuning when the algorithm is far away from the optimal natural frequency and slower tuning when the algorithm is near the optimal natural frequency.

Once the gradient based tuning is complete, the controller continuously monitors the amplitude of the microphone voltage and the excitation frequency to determine when retuning is needed. The flowchart for this tuning algorithm is shown in Figure 9.

## 4. RESULTS

Steady state and transient response tests were performed on the controlled system to evaluate the robustness of the proposed tuning algorithm. The resonator natural frequency range was restricted in software to be between 65 and 160 Hz to avoid possible damage to the resonator wall hinge at the extreme locations.

## 4.1. STEADY STATE RESPONSE OF CONTROLLED SYSTEM

The steady state performance of the controlled system was tested by measuring the steady state microphone voltage amplitudes for discrete excitation frequencies over the operating frequency band of the tunable Helmholtz resonator. This test was used to evaluate the robustness of the tunable Helmholtz resonator over its natural frequency range. A comparison of the noise in the duct system with and without the tunable resonator is shown in Figure 10. To measure the sound pressure spectrum of the system without the tunable resonator, white noise was generated with the loudspeaker and the transfer function between the speaker input and the microphone output was measured. The maximum noise attenuation is 30 dB and occurs at 160 Hz. The minimum noise attenuation is 15 dB and occurs at 80 Hz.

Shown in Figure 11 is a comparison between the noise control realized with the proposed tuning algorithm and the sound pressure spectrum of the acoustic system for several preset natural frequencies. To measure the sound pressure spectrums of the system with preset resonator natural frequencies, white noise was generated with the loudspeaker and the transfer function between the speaker input and the microphone output for fixed Helmholtz resonator wall angles was measured. It is evident that the tuning algorithm is effective in adjusting the cavity volume in order to achieve the optimal noise reduction regardless of the excitation frequency.

## 4.2. TRANSIENT RESPONSE OF CONTROLLED SYSTEM

Transient testing was used to verify the robustness of the tuning algorithm to tuning direction and performance optimization for a time varying excitation frequency. The first transient test involved an instantaneous change in excitation frequency from 65 Hz to 160 Hz. These two excitation frequencies are near the extremes of the frequency range of

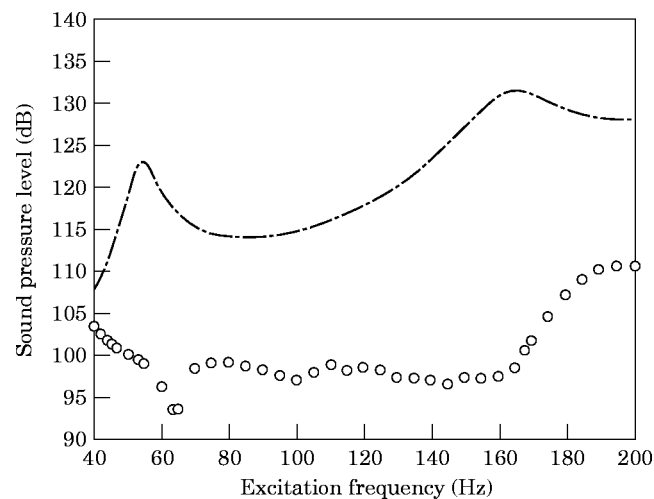


Figure 10. A comparison of the treated and untreated system sound pressure levels. - · - ·, Without resonator; ○, with tunable resonator.

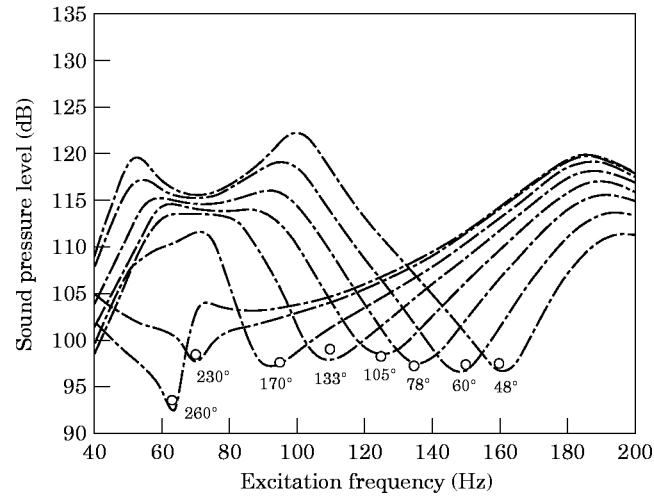


Figure 11. A comparison between the controlled system and the preset resonator wall angles.  $\cdot\cdot\cdot\cdot$ , Fixed resonator wall angles,  $\circ$ , controlled resonator.

the Helmholtz resonator. The change in the excitation frequency occurred 5 s after the beginning of the test. The transient response of the sound pressure level is shown in Figure 12 for both the proposed tuning scheme and a scheme with only open loop control. Shown in Figure 13 is the Helmholtz resonator wall angle measured by the potentiometer for these transient tests. The gradient based tuning achieved an additional 1 dB reduction in the sound pressure level over the strictly open loop scheme. This slight improvement is expected, since the resonator natural frequency is accurately predicted by equation (2) (see Figure 6). However, additional performance improvement would be achieved if the temperature, for example, were to change, thereby changing the speed of sound. In such a case the gradient based tuning strategy would be more influential. The different starting sound pressure levels for the gradient based scheme and the strictly open loop scheme are

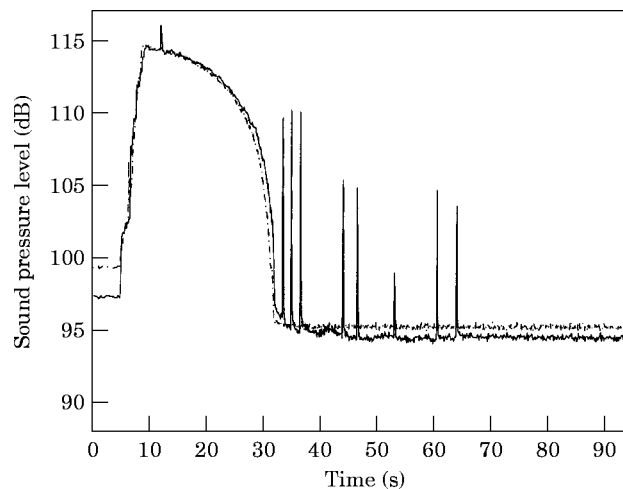


Figure 12. The transient response of the controlled system to excitation change from 65 to 160 Hz.  $\cdot\cdot\cdot\cdot$ , Open loop; —, Open loop, and gradient descent.

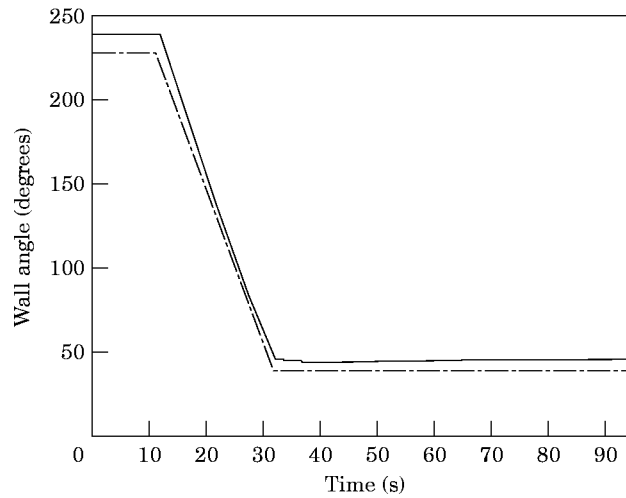


Figure 13. The Helmholtz resonator wall angle for excitation change from 65 to 160 Hz. - - -, Open loop; —, open loop and gradient descent.

the steady state sound pressure levels for each of these schemes for an excitation frequency of 65 Hz.

The time duration for tuning is contingent upon the test hardware, which was not optimized for minimal tuning times. If the tuning time is important, better hardware could be found. The sound pressure spikes shown in Figure 12 were generated by mechanical noises which occurred during the wall adjustments of the gradient based tuning scheme.

An additional transient test was performed for an instantaneous excitation frequency change from 65 Hz to 100 Hz. The transient response of the sound pressure level is shown in Figure 14, and the resonator wall angle measured by the potentiometer is shown in Figure 15. The change in the excitation frequency occurred 5 s after the beginning of the

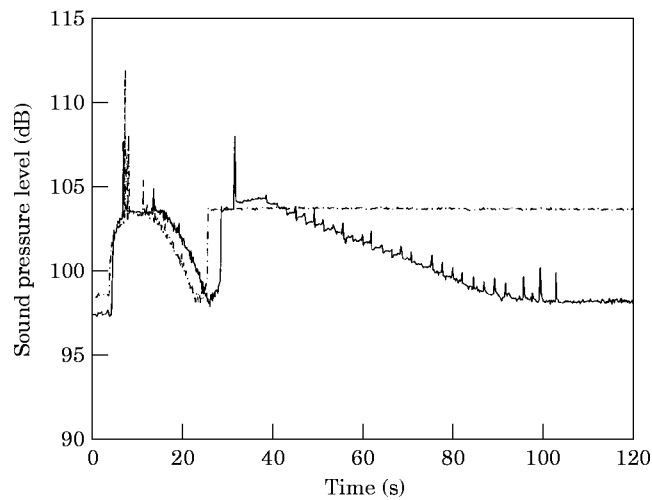


Figure 14. The transient response of the controlled system to excitation change from 65 to 100 Hz. - - -, Open loop; —, open loop and gradient descent.

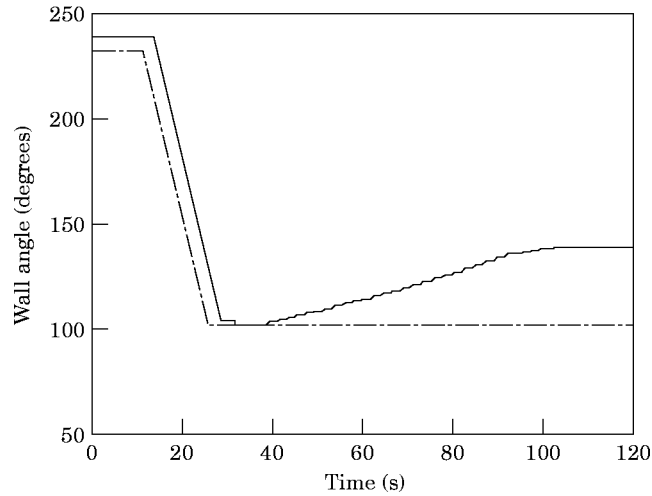


Figure 15. The Helmholtz resonator wall angle for excitation change from 65 to 100 Hz. - - -, Open loop; —, open loop and gradient descent.

test. The 100 Hz excitation frequency was chosen since the open loop control scheme does not accurately predict the required wall position as shown in Figure 6. A 5.5 dB improvement was achieved using the gradient based tuning algorithm. In a similar manner, the effects of variations in air temperature and other environmental conditions would also be minimized with the gradient based approach. Once again, the different starting sound pressure levels for the gradient based scheme and the strictly open loop scheme are the steady state sound pressure levels for each of these schemes for an excitation frequency of 65 Hz. Additional tests of the control algorithm can be found in reference [19].

## 5. CONCLUSIONS

A robust tuning algorithm that ensures optimal performance of an adaptive Helmholtz resonator under changing environmental conditions and excitation frequencies is presented in this paper. The tuning strategy is comprised of the combination of an open loop coarse tuning scheme and a closed loop precise tuning scheme that ensures system convergence to the minimum sound pressure level at the microphone location. A simple lumped parameter model of the Helmholtz resonator is used to implement the open loop tuning portion of the control strategy. Extensive system modeling is not required for this strategy, since the closed loop precise tuning algorithm is used to achieve optimal resonator adjustment. Only one microphone is used to implement the control algorithm. Sound pressure level reductions of up to 30 dB were achieved with the combination of the tunable resonator and the control algorithm.

The main advantages of the adaptive-passive noise control device presented in this paper over active noise control schemes are that the control algorithm is simple and less energy is required for noise reduction (i.e., intermittent motor pulses versus continuous loudspeaker consumption). The main advantage of the tunable Helmholtz resonator over passive devices such as conventional resonators is that the devices will remain optimally tuned despite changes in the excitation frequency and environmental conditions. One disadvantage of the device is that it is limited to tonal noise applications, since only one frequency can be treated.

## REFERENCES

1. U. INGARD 1994 *Notes on Sound Absorption Technology*. Poughkeepsie, NY: Noise Control Foundation. See pp. 7.9–7.13.
2. J. S. ANDERSON and M. BRATOS-ANDERSON 1993 *Noise; Its Measurement, Analysis, Rating and Control*. Brookfield, VM: Ashgate. See pp. 297–300.
3. M. L. MUNJAL 1987 *Acoustics of Ducts and Mufflers with Application to Exhaust and Ventilation System Design*. New York: John Wiley. See pp. 75–78.
4. R. J. BERNHARD, H. R. HALL and J. D. JONES 1992 *Inter-Noise 92*, 427–430. Adaptive–passive noise control.
5. S. M. KUO and D. R. MORGAN 1996 *Adaptive Noise Control Systems—Algorithms and DSP Implementations*. New York: John Wiley. See pp. 53–99.
6. M. C. ALLIE, C. D. BREMIGAN, L. J. ERIKSSON and R. A. GREINER 1988 *Proceedings of the IEEE International Conference on Acoustics, Speech, and Signal Processing 5*, 2598–2601. Hardware and software considerations for active noise control.
7. G. KOOPMANN and W. NEISE 1980 *Journal of Sound and Vibration*. **73**, 297–308. Reduction of centrifugal fan noise by use of resonators.
8. G. KOOPMANN and W. NEISE 1982 *Journal of Sound and Vibration*. **82**, 17–27. The use of resonators to silence centrifugal blowers.
9. E. LITTLE, A. REZA KASHANI, J. KOHLER and F. MORRISON 1994 *ASME DSC Transportation Systems 54*, DE-Vol. 76. Tuning of an electrorheological fluid-based intelligent Helmholtz resonator as applied to hydraulic engine mounts.
10. J. S. LAMANCUSA 1987 *Proceedings of Noise-Con 87*, 313–318. An actively tuned, passive muffler system for engine silencing.
11. P. KRAUSE, H. WELTENS and S. HUTCHINS 1992 *SAE Technical Papers Series, Paper 922088*, 1–11. Advanced design of automotive exhaust silencer systems.
12. P. KRAUSE, H. WELTENS and S. M. HUTCHINS 1993. *Automotive Engineering*. 13–16. Advanced exhaust silencing.
13. H. MATSUHISA, B. REN and S. SATO 1992. *Japan Society of Mechanical Engineers, International Journal 35*, 223–228. Semiactive control of duct noise by a volume-variable resonator.
14. H. MATSUHISA and S. SATO 1990 *Proceedings of Inter-Noise 90*, 1305–1308. Semi-active noise control by a resonator with variable parameters.
15. A. M. McDONALD, S. M. HUTCHINS, J. STROTHERS and P. J. CROWTHER. *International Patent Number W092/15088*. Method and apparatus for attenuating acoustic vibrations in a medium.
16. L. KINSLER, A. FREY, A. COPPENS and J. SANDERS 1982 *Fundamentals of Acoustics*. 201–202, 226–227. New York: John Wiley; third edition.
17. M. W. RYAN 1994 *M.Sc. Thesis, Purdue University*. Adaptive–passive vibration control.
18. M. W. RYAN, M. A. FRANCKEK and R. J. BERNHARD 1994 *Proceedings of Noise Con 94*, 461–466. Adaptive–passive vibration control of single frequency excitations applied to noise control.
19. J. M. DE BEDOUT 1996 *M.Sc. Thesis, Purdue University*. Adaptive–passive noise control with self-tuning Helmholtz resonators.